JVI Journals.ASM.org

Major Histocompatibility Complex Class I Downregulation Induced by Equine Herpesvirus Type 1 pUL56 Is through Dynamin-Dependent Endocytosis

Teng Huang,[a] Maik J. Lehmann,[b] Abdelrahman Said,[a,c] Guanggang Ma,[a] Nikolaus Osterrieder[a]

Institut für Virologie, Freie Universität Berlin, Zentrum für Infektionsmedizin—Robert von Ostertag-Haus, Berlin, Germany[a]; Department of Molecular Parasitology, Humboldt University, Berlin, Germany[b]; Parasitology and Animal Diseases Department, National Research Center, Dokki, Giza, Egypt[c]

ABSTRACT

Equine herpesvirus type 1 (EHV-1) downregulates cell surface expression of major histocompatibility complex class I (MHC-I) in infected cells. We have previously shown that pUL56 encoded by the EHV-1 ORF1 gene regulates the process (G. Ma, S. Feineis, N. Osterrieder, and G. R. Van de Walle, J. Virol. 86:3554–3563, 2012, doi:http://dx.doi.org/10.1128/JVI.06994-11). Here, we report that cell surface MHC-I in EHV-1-infected cells is internalized and degraded in the lysosomal compartment in a pUL56-dependent fashion. pUL56-induced MHC-I endocytosis required dynamin and tyrosine kinase but was independent of clathrin and caveolin-1, the main constituents of the clathrin- and raft/caveola-mediated endocytosis pathways, respectively. Downregulation of cell surface MHC-I was significantly inhibited by the ubiquitin-activating enzyme E1 inhibitor PYR41, indicating that ubiquitination is essential for the process. Finally, we show that downregulation is not specific for MHC-I and that other molecules, including CD46 and CD63, are also removed from the cell surface in a pUL56-dependent fashion.

IMPORTANCE

We show that alphaherpesvirus induces MHC-I downregulation through endocytosis, which is mediated by pUL56. The dynamin-dependent endocytic pathway is responsible for MHC-I internalization in infected cells. Furthermore, we discovered that this endocytic process can be disrupted by the inhibiting ubiquitin-activating E1 enzyme, which is indispensable for ubiquitination. Finally, pUL56 action extends to a number of cell surface molecules that are significant for host immunity. Therefore, the protein may exert a more general immunomodulatory effect.

To achieve productive infection in host cells, viruses have evolved strategies to evade the recognition by the host immune system. Immunity mediated by cytotoxic $CD8^+$ T lymphocytes (CTLs) is of critical importance in the defense against cell-associated pathogens (1). CTLs interact with major histocompatibility complex class I (MHC-I), onto which antigenic peptides are loaded in the endoplasmic reticulum (ER). MHC-I molecules mature while trafficking through the ER and Golgi network before they eventually reach the cell surface (2). Presentation of antigenic peptides derived from viruses and other nonself proteins results in specific sensing by CTLs and ultimate elimination of (infected) cells displaying such peptides. However, a number of viral proteins target the MHC-I antigen presentation pathway, resulting in the downregulation of cell surface MHC-I and immune evasion (reviewed in references 3 and 4).

The adenovirus protein E3-19K was the first identified viral protein shown to block antigen presentation by MHC-I (5). Later, a number of MHC-I downregulators in the *Herpesviridae* were identified, with ICP47 of herpes simplex virus 1 (HSV-1) being the first. ICP47 is a cytoplasmic protein that prevents transport of proteasome-generated peptides into the ER through irreversible blockade of the transporter associated with antigen processing (TAP) (6, 7). Other alphaherpesviruses also encode proteins that reduce the expression of surface MHC-I. Recently, the central role of pUL49.5 in interfering with MHC-I assembly and transport was characterized for pseudorabies virus (PRV), bovine herpesvirus type 1 (BHV-1), and equine herpesvirus type 1 (EHV-1) and type 4 (EHV-4). This ER-resident membrane protein also inhibits TAP activity and delays maturation of MHC-I, because in the absence of antigenic peptides, the trimolecular complex (MHC-I heavy chain, β2-microglobulin, and peptide) cannot be properly assembled (8, 9).

As a member of the genus *Varicellovirus*, EHV-1 is an important pathogen that threatens horse populations worldwide. EHV-1 infection is characterized by upper respiratory disease, neurological disorders, and abortion in pregnant mares (10). It has been known that CTL-based immunity confers protection against EHV-1-induced abortion in mares (11). However, EHV-1 subverts this host defense mechanism by reducing cell surface MHC-I, which may provide an explanation of why vaccination has failed to provide satisfactory protection against infection and also clinical disease. Studies have shown that MHC-I downregulation caused by EHV-1 might be associated with endocytosis and mediated by the expression of an early viral gene(s) (12). Recently, we identified pUL56 of EHV-1 as an early viral protein that plays a dominant role in this process (13). A similar function of the

Received 17 July 2014 **Accepted** 19 August 2014
Published ahead of print 27 August 2014
Editor: K. Frueh
Address correspondence to Nikolaus Osterrieder, no.34@fu-berlin.de.
G.M. and N.O. are joint senior authors.
Supplemental material for this article may be found at http://dx.doi.org/10.1128/JVI.02079-14.

doi:10.1128/JVI.02079-14

TABLE 1 Oligonucleotides used for plasmid construction

Primer	Sequence (5′–3′)[a]
DsRed2-kan Fw	ATCGTACCCATCTACATGGCCAAGAAGCCCGTGC**TAGGGATAACAGGGTAATCGAT**
DsRed2-kan Rv	AAGCTGTCCATGTAGATGGACTTGAACTCCA**CCACCAGTGTTACAACCAATTAACC**
DsRed2-ep Fw	TAGTGAACCGTCAGATCCGCTAGCGCTACCGGTCGCCACC ATGGCCTCCTCCGAGAACGT
DsRed2-ep Rv	GTAAAACCTCTACAAATGTGGTATGGCTGATTATGATCAG CTACAGGAACAGGTGGTGGC
Cav1 Fw	GATCAAGCTTATGTCTGGGGGCAAATACGT
Cav1 Rv	CGCGGATCCC*GAGCGTAGTCTGGGACGTCGTATGGGTA*TATTTCTTTCTGCAGGTTGA
Cav1Y14F Fw	GATCAAGCTTCGATGTCTGGGGGCAAATACGTGGACTCCGAGGGACATCTC***TTC***ACGGTTCCCATCCGGGAACA

[a] Underlined letters indicate restriction sites; bold letters indicate annealing sequences targeting kanamycin; italic letters indicate HA tag sequences; bold italic letters indicate the point mutation corresponding to the 14th amino acid residue of caveolin-1.

pUL56 homologue of EHV-4 was also reported (14), suggesting that MHC-I downregulation caused by pUL56 might be evolutionarily conserved in the genus. However, the mechanism of pUL56 in downregulating cell surface MHC-I remains unknown.

In the present study, we explored the mechanism underlining pUL56-induced MHC-I downregulation in more detail. Our findings can be summarized as follows: (i) cell surface MHC-I is degraded mainly in the lysosomal compartment of infected cells; (ii) relocation of surface MHC-I to lysosomes coincides with the expression of pUL56; (iii) internalization of cell surface MHC-I is dependent on dynamin but does not occur not through clathrin- or caveola-dependent endocytosis; (iv) pUL56-induced MHC-I downregulation requires tyrosine kinase and ubiquitination; (v) the immune cell surface markers CD46 and CD63 are additional targets of pUL56 for degradation. We therefore propose that pUL56 induces degradation of cell surface immune molecules in lysosomes through dynamin-mediated endocytosis in which ubiquitination plays a critical role.

MATERIALS AND METHODS

Cells and viruses. Rabbit kidney (RK13) cells and human HeLa cells were maintained in Earle's minimum essential medium (EMEM) supplemented with 10% heat-inactivated fetal bovine serum (FBS; Biochrom AG), 100 U/ml penicillin and 0.1 mg/ml streptomycin (1% Pen/Strep; Sigma). The equine skin fibroblast cell line NBL6 (ATCC) was maintained in Iscove's modified Dulbecco's medium (Invitrogen) supplemented with 10% FBS, 1% nonessential amino acids (Biochrom AG), and 1% Pen/Strep. RK13 cells were used to propagate and titrate all the viruses in this study.

EHV-1 strain Ab4, constructed previously as a bacterial artificial chromosome (BAC) by insertion of a mini-F sequence in place of the gp2-encoding gene 71 (15), and mutants thereof were used in this study. The pAb4 BAC was maintained in *Escherichia coli* GS1783 (a gift from Greg Smith, Northwestern University, Chicago, IL), and the BAC-reconstituted virus vAb4G and its *ORF1* deletion mutant, vAb4GΔ1, were described previously (13). vAb4G and vAb4GΔ1 both express enhanced green fluorescent protein (EGFP) and allow rapid identification of virus-infected cells. Based on vAb4G and vAb4GΔ1, vAb4 and vAb4Δ1 were generated, in which mini-F sequences containing *egfp* genes were removed and expression of gp2 was restored (13).

To generate Ab4-dsRed2, *egfp* in the mini-F vector sequence of pAb4 was replaced with the *dsRed2* gene using two-step Red-mediated recombination (16). Briefly, a kanamycin resistance gene (*kan*) with an I-SceI restriction site upstream was amplified using the primer pair dsRed2-kan Fw/Rv (Table 1) and cloned into the BstXI site within the *dsRed2* gene present in plasmid pdsRed2-N1 (Clontech). Using the primers dsRed2-ep Fw and dsRed2-ep Rv (Table 1), the entire cassette was amplified by PCR, and the product was electroporated into GS1783 cells harboring pAb4. After the first Red recombination, kanamycin-resistant colonies were screened by restriction fragment analysis. In the second round of Red recombination, the *kan* gene was excised and the resolved clones were analyzed by PCR, sequencing, and restriction fragment analysis. The final construct was transfected into RK13 cells to obtain the recombinant virus Ab4-dsRed2.

Antibodies. Anti-MHC class I monoclonal antibody (MAb) H58A (mouse anti-human MHC class I MAb) was purchased from VMRD. Rabbit anti-EHV-1 pUL56 polyclonal antibodies (PAbs) were designed and produced by GenScript Corporation (NJ, USA) (13). Rabbit antiserum for EHV-1 IR6 was prepared in a previous study (17). A β-actin (13E5) rabbit MAb was obtained from Cell Signaling Technologies. Rabbit PAbs against the hemagglutinin (HA) epitope, LAMP-1, and caveolin-1 were obtained from Abcam. Mouse anti-human CD46 and CD63 MAbs were from BioLegend. Mouse anti-human CD58, CD59, and CD95 MAbs were purchased from Genway Biotech. Alexa Fluor 647-conjugated goat anti-mouse IgG, Alexa Fluor 488-conjugated goat anti-rabbit IgG, and Alexa Fluor 568-conjugated goat anti-mouse IgG were from Invitrogen, while horseradish peroxidase (HRP)-labeled goat anti-rabbit IgG was from Southern Biotech.

Pharmacological inhibitors and flow cytometry. All pharmacological inhibitors used in this study were purchased from Sigma and dissolved in either water or dimethyl sulfoxide (DMSO) depending on the drug and the recommendation of the supplier. The drug concentrations used were 5 μM lactacystin, 150 μM chloroquine, 10 mM ammonium chloride (NH_4Cl), 0.1 to 2 μM bafilomycin A1, 2 to 80 μM dynasore, 0.5 to 10 μg/ml of chlorpromazine, 2 to 50 μg/ml of genistein, 1 to 5 μg/ml of filipin, 2 and 20 μg/ml of nystatin, 10 and 20 mM methyl-β-cyclodextrin (MβCD), and 5 μM and 10 μM PYR41. Pitstop2 was dissolved in DMSO and used at 5 μM and 10 μM, and Pitstop2-Neg (10 μM) was used as a negative control (Pitstop2 and Pitstop2-Neg were kindly provided by Volker Haucke, MDC Berlin-Buch, Germany) (18). The biological functions of each inhibitor are summarized in Table 2. To examine the effect of drugs on MHC-I surface expression after EHV-1 infection, NBL6 cells were infected with vAb4G at a multiplicity of infection (MOI) of 5. After 2 h of incubation, virus was removed, and fresh medium containing different concentrations of drugs was added. After 4 h of inhibition, cells were trypsinized and washed twice with 1× phosphate-buffered saline (PBS) containing 2.5% FBS. Cell surface MHC-I was stained with H58A MAb (1/100), followed by incubation with Alexa Fluor 647-conjugated goat anti-mouse IgG (1/500), and analyzed immediately using a FACSCalibur flow cytometer (Becton-Dickinson). For each sample, at least 10,000 cells were recorded. To stain both cell surface and intracellular MHC-I (total MHC-I), cells were fixed in 3.5% paraformaldehyde (PFA) for 10 min before incubation with antibodies in buffer containing 0.02% saponin (Sigma). Cell death was examined in parallel by staining the cells with propidium iodide (PI). When samples were analyzed in a three-color detection mode, compensation between two contiguous channels was adjusted to subtract the spillover background, as the manufacturer's instructions suggest (BD Biosciences). MHC-I levels are presented as mean fluorescence intensities unless stated otherwise. At least three independent experiments were performed for each treatment condition.

TABLE 2 Summary of inhibitors and their effects on restoration of MHC-I in infected cells

Inhibitor	Targeted pathway	Concn(s)	Specificity	Recovery of MHC-I[a]
Lactacystin	*Proteasome*[b]	5 μM	Inhibition of proteasome activities by modifying threonine residual	−
	Endocytosis[b]			
Chloroquine	Lysosome	150 μM	Induction of lysosomotropic pH elevation to prevent subsequent fusion of endosomes	++
Ammonium chloride	Lysosome	10 mM	Neutralizing the low pH step required for the progression of lysosome	++
Bafilomycin A1	Lysosome	0.1, 0.5, 2 μM	Potent inhibition of acidification by blocking vacuolar proton pump	+
Dynasore	Dynamin mediated	2, 20, 80 μM	Interference with the GTPase activity of the dynamin family	+
Chlorpromazine	Clathrin mediated	0.5, 2, 10 μg/ml	Reshuffling of clathrin and its adaptor protein in the endocytic route	−
Pitstop2	Clathrin mediated	5, 10 μM	Reversible competition for the clathrin-box binding site in terminal domain	−
Genistein	Clathrin independent	2, 10, 50 μg/ml	Tyrosine kinase inhibitor that disrupts the actin network of endocytic site	+
Filipin	Clathrin independent	1, 2, 3, 5 μg/ml	Selectively bound to constitutive cholesterol in caveolae structure	+
Nystatin	Caveola mediated	2, 20 μg/ml	Sequestration of sterol embedded in lipid bilayers	−
Methyl-β-cyclodextrin	Caveola mediated	10, 20 mM	Perturbation of lipid raft synthesis essential for caveolin-dependent endocytosis	−
PYR41	*Ubiquitination*[b]	5, 10 μM	Inhibition of ubiquitination by targeting ubiquitin-activating enzyme (E1)	+

[a] −, no significant effect; +, significant effect; ++, very significant effect.
[b] Bold and italics indicate pathways versus individual endocytosis mechanisms.

Internalization assay. To determine the dynamics of MHC-I on cell surfaces, antibody-based surface labeling was performed as described elsewhere (19). Briefly, mock- or virus-infected cells were incubated on ice with excess amounts (100 μg/ml) of MAb CZ3 (kindly provided by Douglas F. Antczak, Cornell University, USA). After 30 min of gentle rocking, cells were washed with ice-cold PBS three times to remove unbound MAb, and the incubation temperature was shifted to 37°C. At different time points, cells were returned to 4°C and harvested. Following incubation with Alexa Fluor 647-conjugated goat anti-mouse IgG (1/500) for 30 min, cells were analyzed by flow cytometry.

Dominant negative plasmids. EGFP-tagged wild-type (WT) dynamin (DynII) and dominant-negative (DN) dynamin (DynII-K44A) constructs were kindly provided by Mark A. McNiven (Mayo Clinic, Rochester, MN, USA) (20). EGFP-tagged DN Eps15 (DIII) and a control construct (DIIIΔ2) were obtained from Alexandre Benmerah (Hôpital Necker-Enfants Malades, Paris, France) (21). An EGFP-fused WT and DN form of equine caveolin-1 (Cav1) were generated. Briefly, total RNA was extracted from NBL6 cells, and cDNA was obtained using RevertAid H minus reverse transcriptase (Fermentas) and an oligo(dT) primer. WT Cav1 with a HA tag at the C terminus was PCR amplified using the forward primer Cav1 Fw and the reverse primer Cav1 Rv (Table 1). The PCR product was digested with HindIII and BamHI and cloned into pEGFP-N1 vector (Clontech) to generate pCav1-EGFP. To obtain the DN form of Cav1, PCR was performed using primer Cav1Y14F Fw (Table 1) and Cav1 Rv, which introduced an amino acid substitution (tyrosine 14 to phenylalanine [Y14F]) while maintaining the C-terminal HA tag. The PCR product was cloned into pEGFP-C1 (Clontech), resulting in pEGFP-Cav1(Y14F). Correct insertion of the genes into recombinant plasmids was confirmed by DNA sequencing. The expression of recombinant Cav1-EGFP and EGFP-Cav1(Y14F) was confirmed by Western blotting using the protocol described below.

To verify the biological functions of the caveolin-1 constructs, they were electroporated into NBL6 cells. Electroporation was performed using cuvettes with a 4-mm electrode gap and the GenePulser Xcell (Bio-Rad) with the following settings: 260 V, 1,050 μF, and 335 Ω (22). Electroporated cells were resuspended in fresh medium and incubated for 24 h, after which the cells were washed twice with EMEM and kept at 4°C for 30 min in the presence of 0.5 μg/ml Alexa Fluor 647-conjugated cholera toxin B (CTxB) (Invitrogen). Cells were then shifted to 37°C and incubated for 15 min, followed by treatment with citrate-buffered saline (CBS, pH 3.0) for 1 min to remove the unabsorbed remnant of CTxB on the cell surface. After a washing with 1× PBS, cells were fixed with 3.5% paraformaldehyde and inspected with a Zeiss LSM 510 confocal microscope.

To examine whether the DN constructs inhibit pUL56-induced MHC-I downregulation, NBL6 cells were electroporated with either the WT or the DN construct. Twenty-four hours posttransfection, cells were infected with Ab4-dsRed2 at an MOI of 3. At 5 h postinfection (p.i.), cells were trypsinized and cell surface MHC-I was detected by MHC-I MAb H58A and Alexa Fluor 647-labeled goat anti-mouse IgG using a FACSCalibur flow cytometer. Cell surface MHC-I expression was determined in cells that had been gated for both EGFP and DsRed2 positivity after compensation.

Western blot analyses. To determine the expression kinetics of pUL56, NBL6 cells were infected with vAb4G or vAb4GΔ1 at an MOI of 5 and incubated at 37°C for 1 h, and then the cells were treated with CBS for 3 min to deactivate remaining virus on the cell surface. Cells were washed twice with 1× PBS, and cells were collected at different times p.i. (0.5, 1, 1.5, 2, 2.5, 3, 4, and 6 h p.i.) by trypsinization and lysed with radioimmunoprecipitation assay (RIPA) buffer (20 mM Tris, pH 7.5; 150 mM NaCl; 1% Nonidet P-40; 0.5% sodium deoxycholate; 0.1% SDS) containing a protease inhibitor cocktail (Roche) and Benzonase (Novagen). After separation by 12% sodium dodecyl sulfate (SDS)-polyacrylamide gel electrophoresis (PAGE) under reducing conditions, proteins were transferred to polyvinylidene fluoride (PVDF) membranes using the semidry method as previously described (13). After blocking with 5% nonfat dry milk in 1× PBS-T (PBS with 0.05% [vol/vol] Tween 20), the membrane was incubated with pUL56 PAbs (1/500), followed by HRP-labeled goat anti-rabbit IgG. Reactive bands were visualized by enhanced chemiluminescence (ECL Plus; GE Health Care).

To verify the expression of recombinant caveolin-1, plasmids pCav1-EGFP and pEGFP-Cav1(Y14F) were transfected into NBL6 cells by electroporation. At 48 h after transfection, cells were lysed and analyzed by Western blotting using rabbit anti-HA PAb.

Indirect immunofluorescence. NBL6 cells were grown on coverslips coated with 0.5 mg/ml collagen A (Biochrom AG) in double-distilled water (ddH_2O) (pH 3.5) and infected with vAb4 at an MOI of 5. At different times p.i., cells were fixed with 3.5% PFA for 5 min at room temperature (RT), followed by permeabilization with 0.1% saponin. After blocking with 3% bovine serum albumin (BSA) in 1× PBS for 1 h, cells were incubated with a mixture of mouse anti-MHC-I MAb H58A (1/1,000) and rabbit anti-LAMP-1 PAb (1/1,000) or rabbit anti-pUL56 PAb (1/200) for 1 h at RT. After 3 washing steps, cells were incubated with a mixture of Alexa Fluor 568 goat anti-mouse IgG (1/1,000) and Alexa Fluor 488 goat anti-rabbit IgG (1/1,000) for 1 h at RT. After the washes, coverslips were mounted and inspected using a Zeiss LSM 510 confocal microscope. To quantify colocalization, correlation analysis using PSC, a

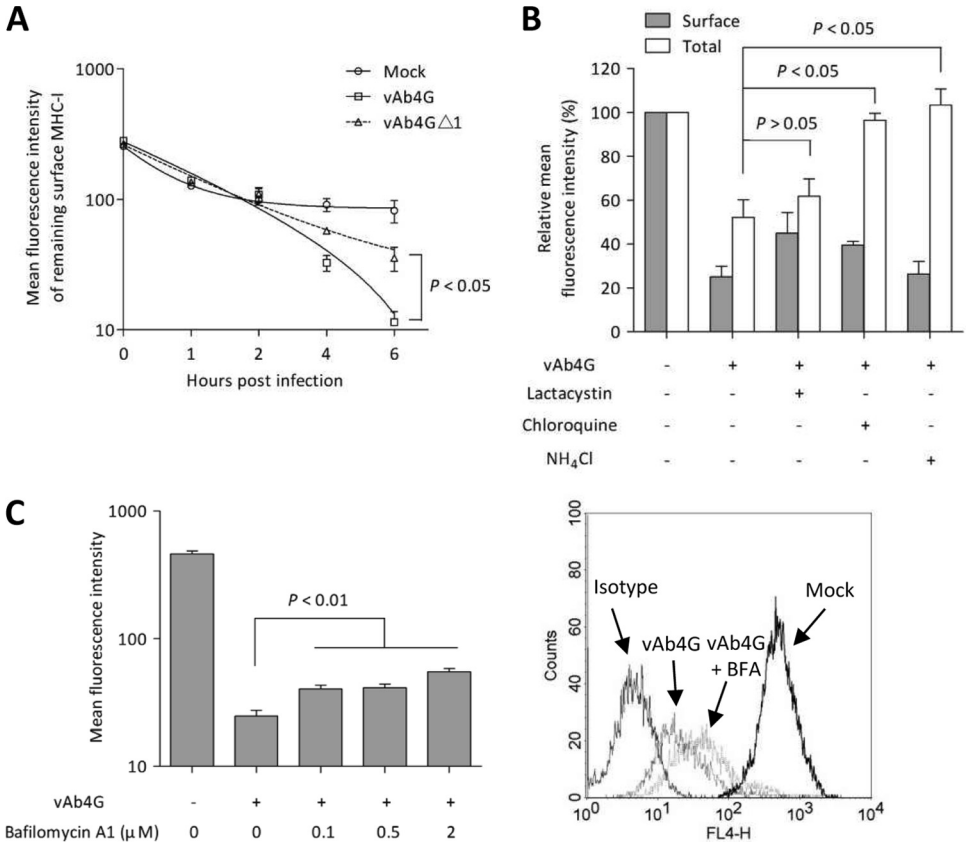

FIG 1 Cell surface MHC-I in EHV-1-infected cells is degraded in lysosomes. NBL6 cells were mock infected or infected with vAb4G or vAb4GΔ1 at an MOI of 5. (A) Cells were incubated on ice for 30 min with excess amounts of MAb CZ3 directed against equine MHC-I. At 0, 1, 2, 4, and 6 h p.i., cells were stained with Alexa Fluor 647-conjugated goat anti-mouse IgG and subjected to analyses using flow cytometry. The trend curves were fitted based on a logarithmic nonlinear regression model. (B) Cells were incubated with the pharmacological inhibitors or 0.1% DMSO as a control. At 6 h p.i., cells were trypsinized and harvested. Monoclonal antibody against MHC-I (H58A) was used to detect cell surface expression of MHC-I. After fixation and permeabilization, total MHC-I levels were assessed. (C) Bafilomycin A1 counteracted the MHC-I downregulation induced by viral infection. Infected cells were treated with the inhibitor at concentrations of 0.1, 0.5, and 2.0 μM, respectively. After 4 h of inhibition, cells were collected and analyzed by flow cytometry. A representative histogram for bafilomycin A1 (BFA) treatment at 2 μM is shown. The data are means ± standard deviations (error bars) from at least three independent experiments. A *P* value of <0.05 indicates a statistically significant difference as determined by one-way analysis of variance (ANOVA).

plugin for ImageJ (http://www.cpib.ac.uk/tools-resources/software/psc-colocalization-plugin), was applied. Areas of interest were analyzed according to the program instructions with a threshold setting at 40. The calculations are presented as Pearson and Spearman correlation coefficients. The Pearson coefficient accounts for the linear relationship between the green and the red channel, whereas the Spearman coefficient describes the nonlinear relationship. For both measurements, the degree of overlap of pixels is associated with values from 0 to 1, where 0 indicates that there is no overlap of pixels and 1 indicates complete overlap.

RESULTS

Cell surface MHC-I in EHV-1-infected cells is redirected to and degraded in the lysosomal compartment. It was proposed that downregulation of MHC-I in EHV-1-infected cells might occur through accelerated endocytosis (12), but the evidence was circumstantial. We sought to address the question of whether surface MHC-I molecules are indeed internalized and where they are redirected. First, we asked whether pUL56 accelerates endocytosis of MHC-I by internalization assays that labeled MHC-I on the cell surface with the CZ3 antibody. A decrease of MHC-I levels was observed at 4 h p.i. in cells infected with vAb4G or vAb4GΔ1 virus, but internalization was significantly slower in cells infected with vAb4GΔ1 lacking pUL56 than in vAb4G-infected cells ($P < 0.05$) (Fig. 1A). We concluded that pUL56 indeed plays a role in MHC-I internalization, and we next began to explore possible endocytic processes that may be responsible for MHC-I downregulation. We started with assessing the role of the proteasome in MHC-I turnover by using the proteasome inhibitor lactacystin. In vAb4G-infected NBL6 cells, both surface and total MHC-I expression was dramatically downregulated at 6 h p.i. With lactacystin treatment, a slight increase of cell surface MHC-I expression in infected cells was observed, while total MHC-I was still detected at low levels that were comparable to those determined in the absence of the inhibitor ($P > 0.05$) (Fig. 1B). This result suggested that the proteasome is not responsible for MHC-I degradation in EHV-1-infected cells.

Lysosomes are responsible for the disposal of many internalized cell surface proteins (23). We speculated that MHC-I from the plasma membrane may be rerouted to lysosomes and degraded in these organelles. To test our hypothesis, chloroquine and ammonium chloride, drugs known to impair lysosomal function, were used. Both drugs are basic compounds that neutralize the vesicular transition from endosomes to lysosomes (24, 25). By

inactivating lysosomal function, we found that cell surface MHC-I was still dramatically downregulated after infection, but total MHC-I levels were restored to those seen in uninfected cells (Fig. 1B), indicating that MHC-I is indeed internalized and degraded in this compartment in EHV-1-infected cells. We also examined the effect of bafilomycin A1, an inhibitor of vacuolar H^+-ATPase that retards the maturation of early endosomes (26). This endocytic inhibitor also mitigated the effect of virus infection on the levels of cell surface MHC-I significantly ($P < 0.05$, Fig. 1C). Overall, the results obtained with the inhibitors clearly demonstrated that endocytosis and lysosomal degradation play a central role in governing the turnover of MHC-I in EHV-1-infected cells.

Trafficking of MHC-I molecules into the lysosome depends on the expression of pUL56. EHV-1 encodes pUL49.5, a type I transmembrane protein that blocks TAP-mediated peptide transport into the ER lumen, where the MHC-I complex is retained as a consequence of the absence of antigenic peptides. With respect to MHC-I downregulation, pUL49.5 and pUL56 are functionally independent (14), suggesting that pUL56 likely targets an alternative pathway to prevent MHC-I presentation. To examine whether pUL56 facilitates lysosomal proteolysis, we recorded the colocalization of MHC-I with lysosomes in a time course experiment by confocal laser scanning microscopy (CLSM). LAMP-1 (lysosome-associated membrane protein 1) was used as a marker to label the lysosomal compartment. At 3 h p.i., MHC-I molecules appeared in the form of vesicles, and colocalization of MHC-I with LAMP-1 was evident (Fig. 2A, top). At 4 h p.i., more MHC-I reactivity was apparent in LAMP-1-containing vesicles, which also seemed to accumulate at the periphery of the nucleus (Fig. 2A, middle). In contrast, infection with the pUL56-negative mutant did not affect the distribution of LAMP-1 in the cytoplasm, and accumulation of MHC-I could not be observed (Fig. 2A, bottom). These findings indicated that degradation of MHC-I is associated with pUL56 expression and redistribution of lysosomal vesicles.

To further assess the relationship between lysosomal degradation of MHC-I and expression of pUL56, colocalization of MHC-I with pUL56 was examined by CLSM. At 3 h p.i., colocalization of MHC-I and pUL56 was apparent (Fig. 2B, top). At 4 h p.i., vesicles that were specifically reactive with the H58A anti-MHC-I and the pUL56 antibodies predominantly clustered in the vicinity of the nucleus (Fig. 2B, middle), whereas no conspicuous relocalization of MHC-I was triggered in the absence of pUL56 (Fig. 2B, bottom). The early expression of pUL56 in vAb4-infected NBL6 cells was confirmed by Western blot analyses. Consistent with our previous report (13), pUL56 was detectable as early as 2 h p.i. With the progress of infection, pUL56 appeared as differently phosphorylated moieties that had increased apparent molecular masses (Fig. 2C). Higher pUL56 expression levels were detected from 4 h p.i., a time when dramatic downregulation of MHC-I on the surface of infected cells was observed (Fig. 1A). Based on the colocalization and expression kinetics data, we surmised that pUL56 is abundantly produced at early times of infection, which allows rapid internalization of surface MHC-I and its subsequent degradation in the lysosomal compartment.

Dynamin-mediated endocytosis is involved in cell surface depletion of MHC-I. Prior to the formation of endosomal vesicles, dynamin is integral in the formation of the invagination structure that ultimately leads to membrane abscission (27). We confirmed the role of dynamin in MHC-I downregulation by chemical interference and the use of dominant negative

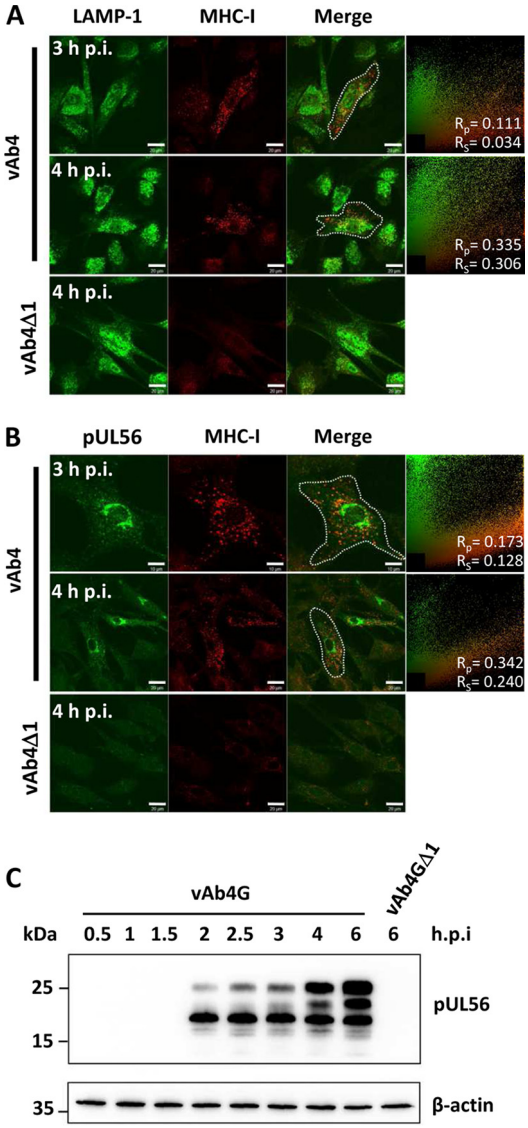

FIG 2 Engulfment of MHC-I molecules is associated with pUL56 expression and followed by lysosomal degradation. (A) Trafficking of MHC-I into the lysosomal vesicles in the presence of pUL56. Lysosome-associated membrane protein 1 (LAMP-1; green) colocalizes with MHC-I (red). Bars, 20 μm. (B) pUL56 (green) and MHC-I (red) colocalize in vAb4-infected cells, while vAb4Δ1 virus deficient in *ORF1* is unable to trigger internalization and aggregation of MHC-I. All images were captured by confocal fluorescence microscopy. The top panels were inspected using a 63× objective. Bars, 10 μm (top) and 20 μm (middle and bottom). Areas for quantitative colocalization analysis were masked with dotted curves. The results are shown in scatter plots, and the Pearson correlation coefficient (R_p) and Spearman correlation coefficient (R_s) are given. Higher values of R_p and R_s indicate stronger colocalization of two proteins. (C) Early expression profile of pUL56 in infection. vAb4G and vAb4GΔ1 at an MOI of 5 were used to infect NBL6 cells, and whole-cell lysates were extracted at the indicated times p.i. After separation using SDS–12% PAGE, proteins were transferred to PVDF membranes and then probed with the pUL56 PAb. β-Actin served as a gel loading control. Molecular mass (kDa) was established by PageRuler Plus from Thermo Scientific.

molecules, respectively. Dynasore is a synthetic inhibitor that specifically targets the GTPase domain and is commonly used to block dynamin-dependent endocytosis (28). At low concentrations of dynasore, levels of cell surface MHC-I were largely

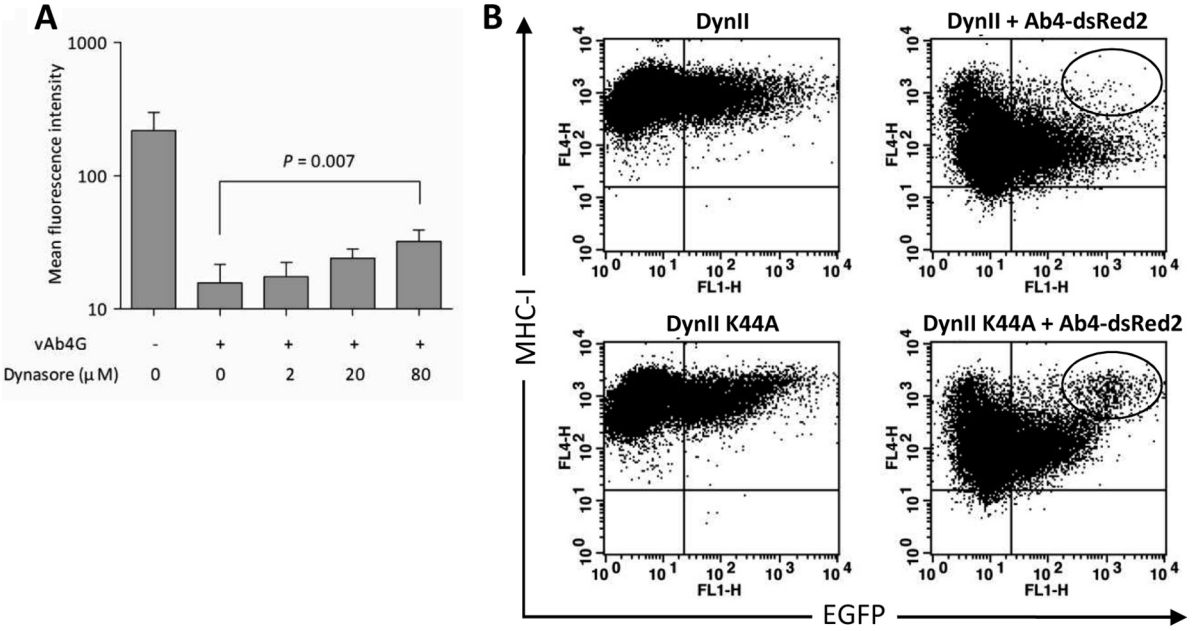

FIG 3 Dynamin-mediated endocytosis regulates cell surface MHC-I. (A) After entry of vAb4G into NBL6 cells, incubation was continued in the presence of increasing amounts of dynasore (2, 20, and 80 μM). Statistical significance was analyzed using one-way ANOVA. (B) NBL6 cells were transfected with WT dynamin (DynII; top) or its DN mutant (DynII-K44A; bottom), both of which are EGFP tagged. Twenty-four hours after transfection, cells were infected with the Ab4-dsRed2 virus. At 5 h p.i., infected cells in which dsRed2 was expressed were gated and analyzed using both EGFP (control or dominant negative) and Alexa Fluor 647 (MHC-I) filters. Differential cell populations are highlighted in the ellipses. Results are representative of three replicates.

unaffected in infected cells; however, they were restored at higher concentrations of the drug. This effect was particularly apparent when cells were incubated in the presence of 80 μM dynasore (Fig. 3A).

DynII-K44A conjugated with EGFP has been confirmed to specifically target dynamin-mediated endocytosis and can be used as a dominant negative form of dynamin (20). To allow dual-color fluorescence detection, an EHV-1 mutant expressing dsRed2 as a marker of infection (Ab4-dsRed2) was generated. MHC-I downregulation induced by Ab4-dsRed2 was indistinguishable from that induced by vAb4G or vAb4 (data not shown). Before infection with Ab4-dsRed2, NBL6 cells were transfected with plasmids expressing WT (DynII) or DN (DynII-K44A) dynamin. The sizes of cell populations expressing DynII and DynII-K44A were largely identical at 24 h after transfection, and no difference in cell surface MHC-I levels was observed in uninfected cells transfected with the WT or DN DynII (Fig. 3B, left). In infected cells (5 h p.i.), cell surface MHC-I expression was analyzed in the cell population expressing both EGFP and dsRed2. In the presence of DynII-K44A, expression of cell surface MHC-I in infected cells was clearly restored (Fig. 3B, right), while WT DynII had no effect. We concluded from the data that EHV-1 enhances MHC-I internalization via dynamin-meditated endocytosis.

Clathrin is not required for surface MHC-I uptake. The best-studied endocytic pathways include clathrin- and caveola-mediated endocytosis. To examine which endocytic pathway is responsible for pUL56-mediated MHC-I downregulation, the role of the clathrin-mediated endocytosis was assessed. In the first set of experiments, we used chlorpromazine, a drug commonly used for inhibiting clathrin-mediated endocytosis (29). In the presence of chlorpromazine, the levels of MHC-I on the surface of infected cells remained as low as those in cells without treatment. With higher concentrations, there was still no significant restoration of MHC-I levels (Fig. 4A). To further examine the role of the clathrin-dependent pathway, we included Pitstop2, a novel inhibitor that blocks clathrin-mediated endocytosis by selectively binding to the terminal domain (TD) of clathrin (18). Consistent with the results obtained with chlorpromazine treatment, MHC-I levels in vA4G-infected cells were not restored after treatment with Pitstop2 and were indistinguishable from those after treatment with Pitstop2-Neg (Fig. 4B).

A dominant negative Eps15 mutant fused to EGFP has been shown to cause substantial delay of clathrin-mediated uptake processes (21, 30). We included this more specific construct to corroborate our findings using the chemical inhibitors. At 24 h after transfection, approximately 40% of NBL6 cells expressed either the control (DIIIΔ2) or the dominant negative form of the protein (DIII). Expression levels of cell surface MHC-I after transfection with either construct were virtually identical (Fig. 4C, left). Upon infection with Ab4-dsRed2 (MOI = 3), DIII had no impact on the inhibition of MHC-I downregulation (Fig. 4C, right), as the levels of surface MHC-I between control cells and those treated with the DN form were not significantly different. Collectively, these results suggested that internalization of MHC-I does not rely on clathrin-mediated endocytosis.

Inhibition of caveola-mediated endocytosis does not affect internalization of MHC-I. Like clathrin-mediated endocytosis, caveolar internalization is another well-characterized dynamin-dependent endocytic pathway, which is initiated by invagination of smooth patches of plasma membrane where cholesterol and sphingolipids are abundant (31). Numerous inhibitors have been reported to effectively block caveolar maturation, including genistein (31), filipin (32), nystatin (33), and MβCD (34). Treatment of cells with genistein resulted in a significant increase of cell surface

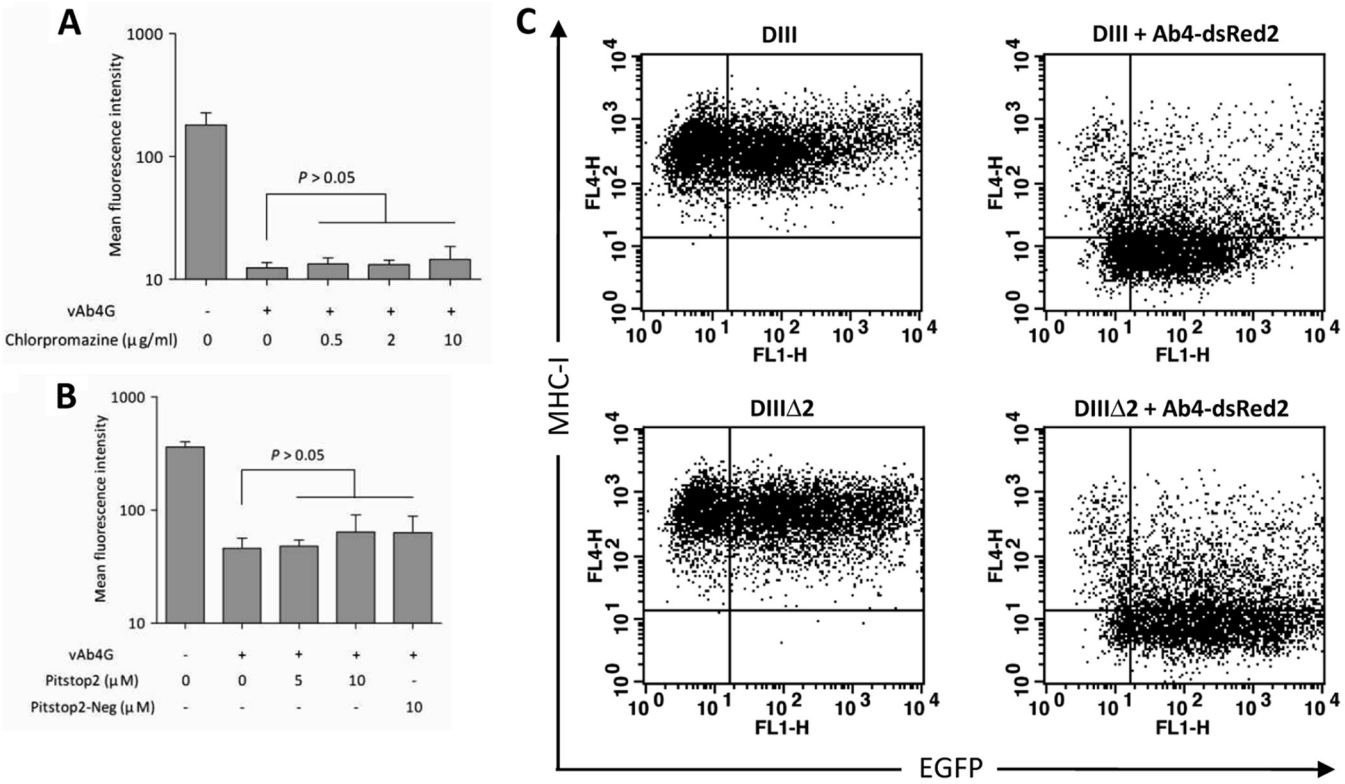

FIG 4 Clathrin-mediated endocytosis is not essential for MHC-I downregulation. (A) NBL6 cells were mock infected or infected with vAb4G in the presence of chlorpromazine (0.5, 2, or 10 μg/ml), an inhibitor commonly used to prevent clathrin recycling. (B) Infected cells were incubated with Pitstop2 at 5 μM or 10 μM. Pitstop2-Neg, a structural analogue of Pitstop2, was used as a control at 10 μM. Similar to chlorpromazine, no effects of Pitstop2 on virus-induced MHC-I downregulation were evident. One-way ANOVA was applied, and a *P* value of >0.05 indicates that the difference is not significant. (C) Effect of the dominant negative Eps15 mutant. NBL6 cells were electroporated with equal amounts of pEGFP-DIIIΔ2 or pEGFP-DIII plasmids and then cultured for 48 h. At 5 h p.i., infected cells expressing dsRed2 were gated and further examined by analyzing the mean fluorescence intensity of GFP (control or dominant negative Eps15) and Alexa Fluor 647 (MHC-I). Neither the WT nor the DN form restored the cell surface expression of MHC-I. Student's *t* test was performed, and no statistical significance between the WT and the DN groups was seen. The dot plots are representative of three independent tests.

MHC-I in infected cells in a dose-dependent manner (Fig. 5A). Therefore, we concluded that virus-mediated endocytosis of MHC-I depends on tyrosine kinase activity. We then tested the role of cholesterol in governing MHC-I internalization by treatment with filipin. In the presence of filipin, particularly at higher concentrations, the recovery of internalized MHC-I was significantly increased compared to that in untreated cells or cells treated with lower concentrations ($P < 0.05$) (Fig. 5B). Thus, membrane-bound cholesterol seems to be involved in allowing the uptake of cell surface MHC-I during EHV-1 infection.

There are multiple factors that control caveolar endocytosis, and we used two additional drugs that interfere with different constituents of caveolar structures. When cells were incubated with nystatin after infection, the levels of MHC-I remained as low as those in untreated cells (Fig. 5C). Similarly, MβCD was unable to prevent virus-induced MHC-I downregulation in infected cells at different concentrations (Fig. 5D). It was not entirely surprising to see differences between the four drugs with respect to MHC-I internalization, because they have different molecular targets and interfere with different signaling pathways. Some of the drugs are known to be pleiotropic and affect other endocytic pathways as well; for example, nystatin and MβCD also interfere with the clathrin pathway (33, 35). In summary, however, the results obtained with chemical inhibitors suggest that MHC-I downregulation requires the activity of tyrosine kinase and is dependent on cholesterol, as deduced from the effects of genistein and filipin treatments, respectively. In contrast, sterol binding and lipid raft integrity seem to not be required, as nystatin and MβCD treatments did not affect virus-induced internalization of MHC-I.

In order to further substantiate the role of caveolar endocytosis, a more specific tool in the form of a DN caveolin-1 (Cav1) mutant was employed. We altered the 14th amino acid residue of Cav1 by PCR-based mutagenesis and replaced the tyrosine with a phenylalanine residue (Y14F) (36, 37). To facilitate detection of proteins by flow cytometry, both the WT and the DN mutant were fused to EGFP and tagged with an HA epitope (Fig. 6A). WT Cav1 was positioned upstream of EGFP (Cav1-EGFP), while the DN Cav1 construct containing the Y14F mutation was positioned downstream of EGFP [EGFP-Cav1(Y14F)]. We reasoned that the N-terminal fusion of Cav1 to EGFP together with the Y14F substitution would ensure the desired dominant negative effect, because caveolar uptake processes can be blocked by N-terminally tagged Cav1 (38). Expression of both forms of Cav1 was readily detectable by Western blot analysis in NBL6 cell lysates (Fig. 6B). The effect of EGFP-Cav1(Y14F) was then evaluated by confocal imaging. Inhibition of caveolar endocytosis was noticeable, as the uptake of cholera toxin B (CTxB) was strongly attenuated in cells transfected with the plasmid expressing EGFP-Cav1(Y14F)

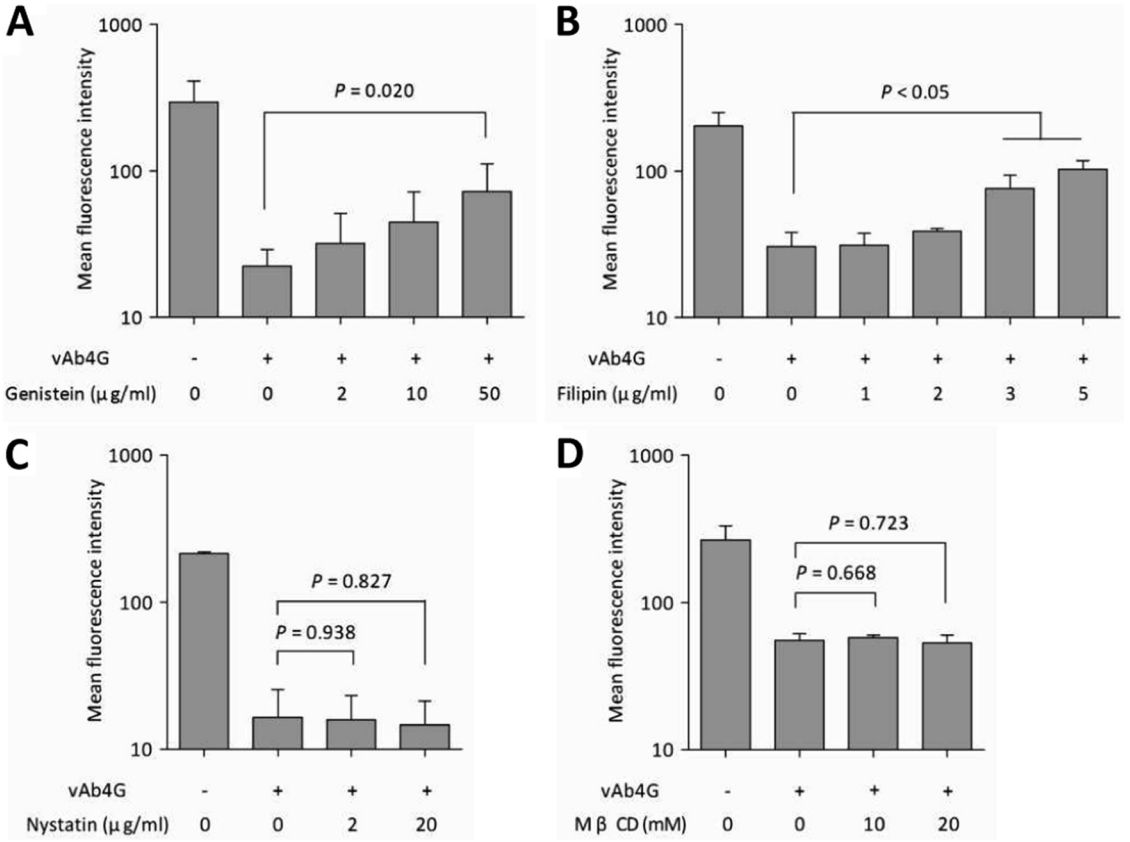

FIG 5 Chemical inhibition of clathrin-independent endocytic pathways. After infection with vAb4G, NBL6 cells were replenished with fresh medium containing genistein at 2, 10, and 50 μg/ml (A), filipin at 1, 2, 3, and 5 μg/ml (B), nystatin at 2 and 20 μg/ml (C), and methyl-β-cyclodextrin (MβCD) at 10 and 20 mM (D). After 4 h of incubation, cells were processed for cell surface MHC-I labeling, and the mean fluorescence intensity of the populations was determined by flow cytometry. Values are expressed as means ± standard deviations (error bars) from at least three independent experiments. One-way ANOVA was used to analyze the statistical difference between groups.

(Fig. 6C). Furthermore, cell surface expression of MHC-I was analyzed in cells overexpressing either of the two forms of Cav1. In the absence of virus infection, overexpression of Cav1-EGFP or EGFP-Cav1(Y14F) did not alter levels of MHC-I on the cell surface (Fig. 6D, left). Likewise, at 5 h p.i., virus-induced downregulation of MHC-I was not affected, regardless of whether the wild-type or mutant form of Cav1 was used (Fig. 6D, right). Also, by using CLSM, we did not detect specific colocalization of caveolin-1 and MHC-I in infected cells (data not shown). We concluded from these experiments that caveolar endocytosis is not involved in MHC-I downregulation mediated by EHV-1.

Ubiquitination is essential for modulating cell surface levels of MHC-I in infected cells. It is known that overexpression of the gammaherpesvirus (Kaposi's sarcoma-associated herpesvirus [KSHV])-encoded ubiquitin E3 ligases K3 and K5 will reduce the levels of MHC-I at the cell surface. This process is mediated by linkage of polyubiquitin chains at lysine 63 (K63 polyubiquitination), which is sufficient to activate endocytosis (39). Given that HSV-2 pUL56 strongly increases ubiquitination of host E3 ligase Nedd4 (40), we speculated that downregulation of MHC-I caused by EHV-1 pUL56 may be dependent on ubiquitination. To test this hypothesis experimentally, infected cells were incubated with PYR41, which interferes with ubiquitination by E1 blockade (41). Incubation of infected cells with 10 μM PYR41 resulted in recovery of cell surface levels of MHC-I at 4 h p.i. compared to untreated cells (Fig. 7A and B). We ruled out the possibility that inhibition of the ubiquitination machinery might impair the expression of pUL56. Upon PYR41 treatment, pUL56 and the early viral protein IR6 (pIR6) remained stable in infected cells. In contrast, elevated MHC-I levels were observed in the presence of the inhibitor (Fig. 7C). We concluded from the results of this experiment that MHC-I downregulation and degradation caused by EHV-1 require ubiquitination, more specifically, an interaction between EHV-1 pUL56 and components of the cellular ubiquitination machinery.

Downregulation of additional cell surface markers by pUL56. Finally, we determined if pUL56-mediated internalization was specific to MHC-I. To this end, cell surface expression of a number of cell surface markers, specifically, CD46, CD58, CD59, CD63, and CD95, was analyzed. All the targeted molecules play critical roles in modulation of host innate or adaptive immunity. CD46 negatively regulates the pathways for complement activation (42), while CD58 and CD59 facilitate the adhesion and activation of T cells (43). Being a costimulatory factor, CD63 is required for the steady activation and proliferation of T cells (44). CD95, best known as Fas receptor, initiates apoptosis when the target cells are recognized by CTLs (45). Because the available antibodies show exclusive reactivity with human and murine but

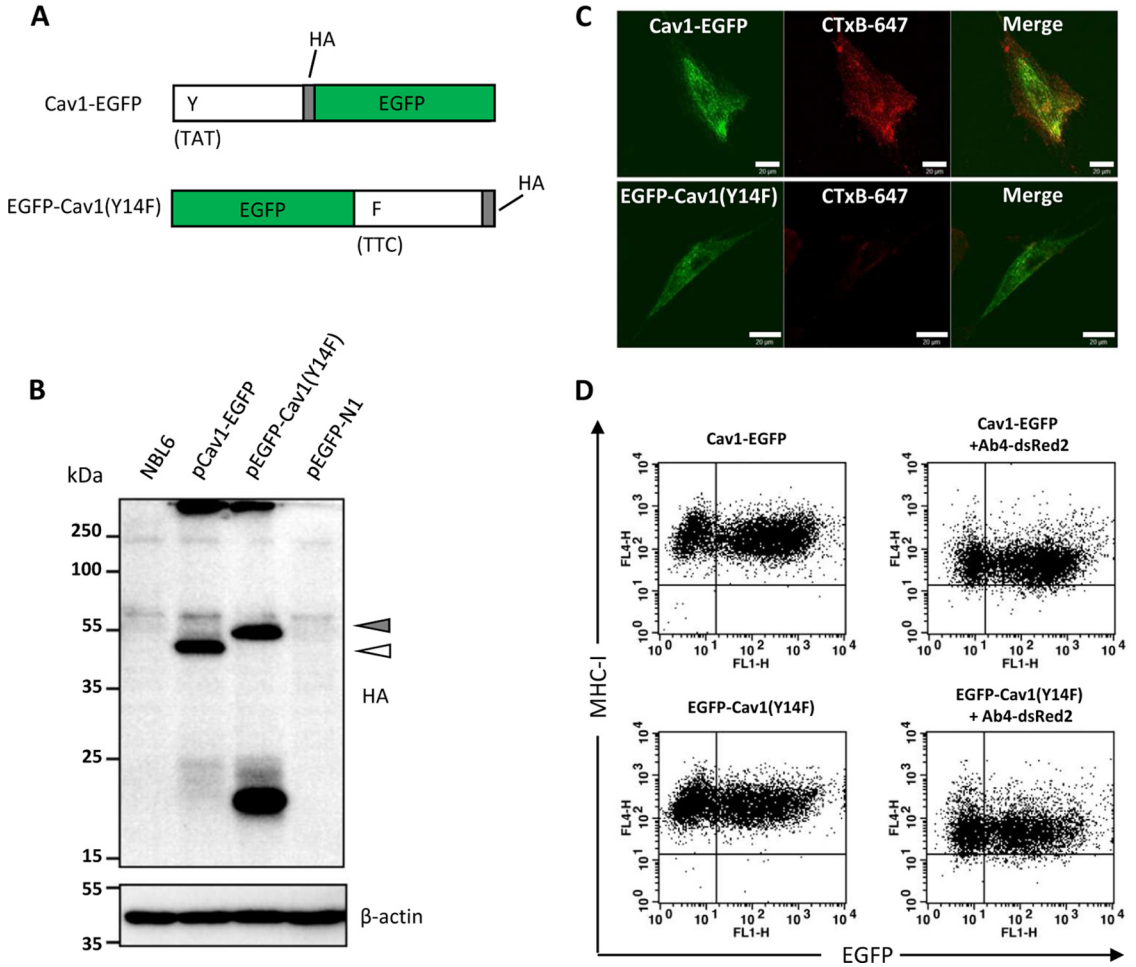

FIG 6 MHC-I downregulation is independent on caveola-mediated endocytosis. (A) Schematic representation of two the forms of caveolin-1 used here, Cav1 (WT) and Cav1(Y14F) (DN), fused to the amino and carboxy termini of EGFP, respectively. (B) Expression of caveolin-1 constructs. At 48 h after transfection, whole-cell lysates were subjected to separation by SDS–12% PAGE followed by Western blot analysis. Specific bands corresponding to the WT (white triangle) or DN (gray triangle) proteins were detected using rabbit anti-HA MAb. β-Actin was used as a loading control. PageRuler Plus from Thermo Scientific was run as a molecular ladder. (C) Inhibition of caveola-mediated endocytosis by the DN mutant. EGFP-Cav1(Y14F) (green) effectively blocked the engulfment of cholera toxin B (CTxB), resulting in the reduced intensity of Alexa Fluor 647 (red). Bars, 20 μm. (D) MHC-I downregulation is not affected by expression of either the WT or the DN mutant after infection. After gating with dsRed2, the infected cells were analyzed by flow cytometry for expression of EGFP and MHC-I. Student's *t* test was performed, and no statistical significance between the WT and the DN groups was seen. Representative dot plots from triplicate assays are presented.

not equine CD molecules, our experiments were conducted using HeLa cells in which MHC-I downregulation dependent on pUL56 had previously been documented (13). For testing each marker, HeLa cells were infected with vAb4G or vAb4GΔ1, the mutant devoid of pUL56. At 24 h p.i., cell surface levels of each marker were analyzed by flow cytometry and plotted as mean fluorescence intensity in histograms. Of the selected markers, pUL56 induced a significant reduction of CD46 and CD63, whereas it did not affect the levels of CD58, CD59, or CD95 (Fig. 8). On the basis of these data, we concluded that pUL56 is able to reduce cell surface levels of molecules other than MHC-I and, hence, may have a more general effect on immunomodulatory molecules in infected cells.

DISCUSSION

Over the past 2 decades, a number of viral inhibitors targeting different stages of MHC-I presentation have been characterized (46). The majority of such inhibitors were found in herpesviruses, although their mechanisms of action vary greatly. Recently, we discovered that pUL56, encoded by the gene *ORF1* of EHV-1, affects MHC-I expression (13). Phylogenetic analyses reveal that pUL56 is conserved in many alphaherpesviruses and that the pUL56 homologue of EHV-4 also downregulates MHC-I at the cell surface (14). It was speculated that loss of cell surface MHC-I is induced by endocytosis in the early stages of EHV-1 infection (12), and here, we investigated the putative relationship between pUL56 and endocytosis that might result in the reduction of MHC-I on the cell surface. By using inhibitors that disrupt endosomal or lysosomal function, we initially determined that endosomal acidification and lysosomal proteolysis govern the fate of internalized MHC-I. This finding was further corroborated by confocal microscopy showing that MHC-I colocalized with the lysosome marker LAMP-1.

Endocytosis is an important intracellular transport mechanism that initiates signal transduction and internalization of a

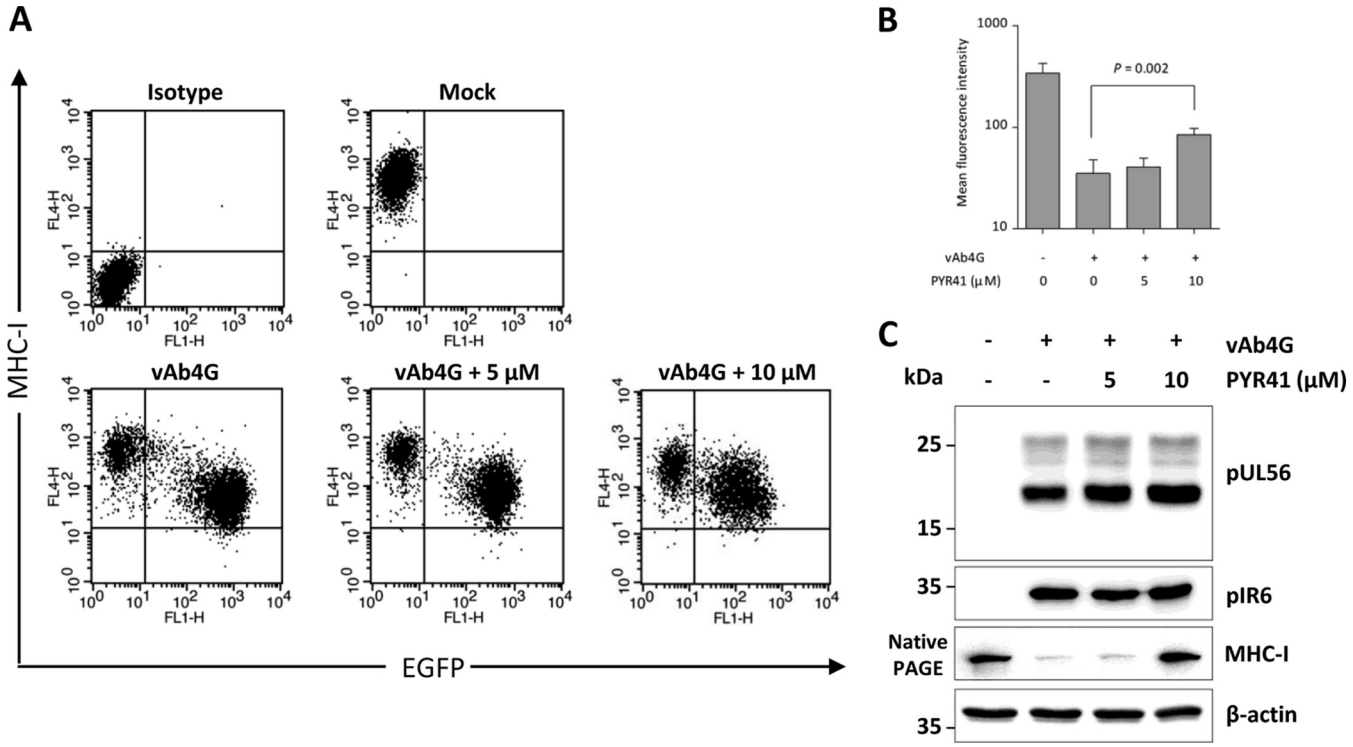

FIG 7 Ubiquitination affects cell surface MHC-I expression in EHV-1-infected cells. (A) Ubiquitination was blocked by PYR41, an E1 inhibitor. NBL6 cells were mock infected or infected with vAb4G for 2 h; afterwards, inhibitor at 5 μM or 10 μM was applied. At 4 h of inhibition, the levels of cell surface MHC-I were determined by flow cytometry. (B) The overall inhibitory effects are shown as dot plots and converted into a bar chart to quantitatively compare mean fluorescence intensities obtained with the treatments. Data analyses were performed using ANOVA. (C) PYR41 reduces MHC-I degradation but does not affect the expression of pUL56. At 4 h p.i., cell lysates were prepared with RIPA buffer and fractionated using SDS–12% PAGE. The expression levels of pUL56 and pIR6 were detected by Western blotting. For MHC-I detection, cell lysates were separated by nondenaturing 12% PAGE, and the blot was probed with anti-MHC-I MAb CZ3. β-Actin was included as a gel loading control.

number of nutrients, lipids, membrane proteins, and pathogens (27). The endocytic pathways that allow infectious entry have been extensively studied for a number of viruses (47); however, it is less well understood how viruses induce endocytosis of key immune-related receptors to achieve immune evasion. Notable exceptions are the KSHV K3 and K5 proteins, which promote MHC-I endocytosis in infected cells. It was shown in transiently transfected cells that these two virus-encoded enzymes directly increase endocytic activity and lead to the uptake of MHC-I molecules from the cell surface (19). Likewise, the HIV Nef protein was shown to downregulate MHC-I through an endocytic pathway (48), which may imply that enhancing endocytosis as a means of preventing or reducing presentation of antigenic (viral) peptides by MHC-I might be evolutionarily conserved among many viruses.

We were able to demonstrate here that EHV-1 pUL56 colocalizes from 4 h p.i. with MHC-I-containing vesicles and the lysosomal marker LAMP-1 in infected cells. This colocalization correlates with decreased cell surface MHC-I levels. The results, therefore, suggest that it is indeed pUL56 that mediates the trafficking of MHC-I molecules to lysosomes for degradation. The two known viral MHC-I inhibitors encoded by alphaherpesviruses, ICP47 and pUL49.5, prevent translocation of antigenic peptide into the ER and formation of the trimolecular complex. Specifically, ICP47 is present in the cytoplasm and exhibits high affinity to TAP, which results in functional inactivation of peptide transport into the ER (49, 50). For pUL49.5, although it also restricts the supply of peptides to the ER, homologues in different viral species are mechanistically diverse. For example, BHV-1 pUL49.5 reduces TAP stability by promoting its proteasomal degradation (8), whereas pUL49.5 of EHV-1 and -4 inhibit the recruitment of ATP, which is indispensable for TAP activity (9). Unlike ER-based interference with MHC-I maturation, pUL56 is predominantly localized to the Golgi apparatus and endosomal vesicles. It does not perturb peptide transport to the ER (13, 14), and its mechanism of action is clearly distinct from those of ICP47 and pUL49.5. Therefore, pUL56 has a novel mode of action with respect to MHC-I downregulation in members of the *Alphaherpesvirinae* and functions more like gammaherpesviral K3 and K5 by interfering with endocytosis.

Based on their constituent elements, endocytic pathways are classified into categories that include clathrin-, caveola-, and Arf6-dependent endocytosis as well as phagocytosis and macropinocytosis (51); however, a growing body of evidence now suggests that unidentified endocytic pathways might exist, and thus the classification scheme has been simplified by discriminating only between clathrin-dependent endocytosis (CDE) and clathrin-independent endocytosis (CIE) (52). Endocytosis inhibitors are commonly used to investigate endocytic pathways responsible for homeostasis of cell surface proteins, but attention should be given to their possibly pleiotropic effects (35). Given that the turnover of cell surface proteins is dynamically regulated under normal phys-

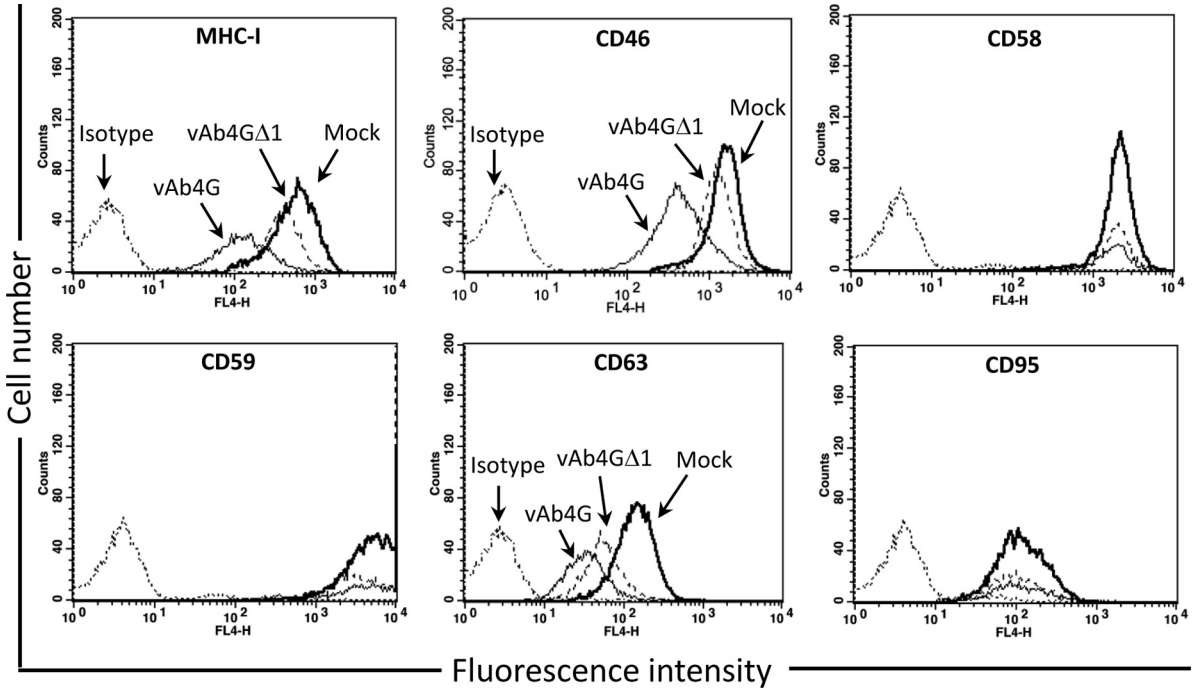

FIG 8 A broader range of surface markers is decreased during EHV-1 infection in a pUL56-dependent fashion. HeLa cells were mock infected (black solid line) or infected with vAb4G (gray solid line) or vAb4GΔ1 (black dashed line). Unspecific binding of antibodies was controlled for by staining with corresponding isotype antibodies (gray dashed line). At 24 h p.i., all cells were sampled and incubated with monoclonal primary antibodies against MHC-I, CD46, CD48, CD58, CD59, CD63, and CD95. Alexa Fluor 647-conjugated goat anti-mouse IgG was used as a secondary antibody. Samples were detected by flow cytometry. The FL4-H axis refers to the fluorescence intensity of the given surface markers. Downregulation of MHC-I, CD46, and CD63, but not that of other markers, was rescued by abrogation of *ORF1*. The histograms are representative of two independent tests.

iological conditions, we tested the influence of our inhibitors on the metabolism of MHC-I, which might distort the interpretation of our results in infected cells. Except for the significant MHC-I reduction seen with the treatment of chloroquine, the other reagents used showed no or very little effect on the presence of MHC-I on the cell surface of mock-infected cells (see Fig. S1 in the supplemental material), ensuring that they target only MHC-I in infected cells. With inhibition of virus-induced MHC-I downregulation by chlorpromazine and Pitstop2 as well by dominant negative molecules, we demonstrated that MHC-I downregulation is not through the CDE pathway. This observation for EHV-1 differs from that for KSHV, where the K3 protein interferes with the classical CDE pathway (39), while a unique Arf6-dependent pathway is targeted by HIV-1 Nef to divert mature cell surface MHC-I to lysosomes for degradation (48). Despite the differences, lysosomes are the ultimate cellular compartment where degradation of MHC-I occurs in the case of KSHV, HIV-1, and EHV-1.

Caveola-dependent endocytosis is considered an important CIE pathway. Along with the involvement of dynamin, caveolin-1 is primarily responsible for the formation of the flask-shaped caveolae (53). Moreover, tyrosine kinase activity is necessary for the aggregation and fusion of caveolae or caveolar vesicles (54). Therefore, it is not surprising that a number of viruses gain access to host cells by nonclassical endocytic pathways that are all dependent on the action of dynamin and tyrosine kinases but differ in other factors involved (55–58). Here, we studied the role of caveola-dependent endocytosis in virus-induced MHC-I downregulation. Despite the various effects of four inhibitors for CIE, transfection of a specific dominant negative form of caveolin-1 was unable to rescue cell surface expression of MHC-I, suggesting that caveola-dependent endocytosis is not involved in MHC-I internalization. In contrast, we found that the decrease of surface MHC-I was remarkably attenuated when the action of dynamin was inhibited with dynasore or a dominant negative form of dynamin. These findings led us to conclude that MHC-I downregulation is associated with dynamin, which facilitates vesicle scission at the plasma membrane and as such is integral to many endocytic pathways (59, 60). To our knowledge, our report describes the first example of an alphaherpesvirus that downregulates cell surface MHC-I through an endocytic pathway that is associated with dynamin but unrelated to clathrin and caveolae. However, there might be another unknown viral protein(s) that can drive MHC-I downregulation through endocytic processes, as knockout of pUL56 alone cannot completely prevent endocytosis of MHC-I mediated by EHV-1 infection.

Ubiquitination determines the destiny of endocytosed membrane proteins (61). On the one hand, the formation of vesicles at different stages of endocytosis requires mono- or polyubiquitination (62). On the other hand, the nature of ubiquitin linkage to lysine results in cargo sorting and degradation either in the proteasome or in the lysosome (63). KSHV K3 and K5 are E3 ubiquitin ligases which directly bind to membrane substrates and trigger endocytosis (39, 64). In the case of HSV-2, pUL56 is able to increase ubiquitination of the E3 ligase Nedd4. This interaction is thought to affect protein sorting or vesicle trafficking but does not affect virus release, as originally surmised (65). Here, EHV-1 pUL56, which is structurally similar to its HSV-2 orthologue, was shown to direct MHC-I molecules for lysosomal degradation.

This process is greatly affected when ubiquitination is chemically blocked. It is therefore tempting to speculate that the function of pUL56 depends on its interaction with an E3 ligase, a hypothesis that we are currently testing.

To address the specificity of pUL56 action, several other cell surface markers were screened in this study. We found that pUL56 can reduce the expression of CD46 and CD63 on the cell surface. CD46 is critical for efficient T cell responses and bridges between the complement system and cellular immunity (66); for instance, expression of CD46 facilitates destruction of the cells infected with measles virus by CTLs, a process that depends on MHC-I antigen presentation (67). CD63 is a membrane protein containing four transmembrane domains (tetraspanin) which is widely distributed on endosomal membranes and known to modulate immune signaling pathways (68, 69). In dendritic cells, for example, intracellular transport of CD63 is associated with antigen presentation by MHC-II (70). The implication of pUL56 in downregulating CD46 and CD63 may suggest that it functions as a more promiscuous immune modulator, a notion that is supported by the results obtained in equids infected with the Ab4 mutant unable to express the protein (71).

Removal of cell surface MHC-I seems a wise strategy for persistent infection, as CTLs would be unable to eliminate infected cells due to a failure to recognize antigens. However, cells devoid of surface MHC-I are unlikely to survive and might be subject to clearance by natural killer (NK) cells. KSHV K5 targets other surface molecules to counteract the threat from NK cells. Along with CD31, CD86, CD144, CD166, and intracellular adhesion molecule 1 (ICAM1) (64), KSHV K5 also downregulates activation-induced C-type lectin (AICL), MHC-I polypeptide-related sequence A (MICA), and MICB, which are required for NK cell lysis (72, 73). Whether pUL56 targets these surface molecules sensed by NK cells remains to be explored.

In this study, we investigated the pathway by which pUL56 induces downregulation of cell surface MHC-I. The endocytic process responsible for MHC-1 removal from the cell surface is mediated by dynamin but not clathrin or caveolae. Importantly, tyrosine kinase activity and membrane-bound cholesterol are required for MHC-I endocytosis as is ubiquitination. The latter may imply that pUL56 function is dependent on the E3 ligase activity. Since pUL56 is able to regulate other cell surface molecules, it may have a more comprehensive role in regulation of the immune response to infection. Future studies will focus on how pUL56 interacts with ubiquitination and the yet-unidentified viral protein(s) it needs to carry out its functions.

ACKNOWLEDGMENTS

We thank Walid Azab for helpful suggestions on inhibitors and maintenance of equine cells. We express gratitude for the Pitstop2 inhibitors, kindly provided by Volker Haucke from the Leibniz-Institut für Molekulare Pharmakologie (FMP), Berlin-Buch, Germany, and the anti-MHC MAb CZ3, provided by Douglas F. Antczak (Cornell University, USA). We also gratefully acknowledge the dominant negative mutants kindly provided by Mark A. McNiven (Mayo Clinic, Rochester, MN, USA) and Alexandre Benmerah (Hôpital Necker-Enfants Malades, Paris, France).

T.H. was supported by a grant from the China Scholarship Council. This study was financed by DFG grant OS143/3-1 and unrestricted funds of Freie Universität Berlin to N.O.

REFERENCES

1. **Wong P, Pamer EG.** 2003. CD8 T cell responses to infectious pathogens. Annu.Rev.Immunol.**21:**29–70.http://dx.doi.org/10.1146/annurev.immunol.21.120601.141114.
2. **Peaper DR, Cresswell P.** 2008. Regulation of MHC class I assembly and peptide binding. Annu. Rev. Cell Dev. Biol. **24:**343–368. http://dx.doi.org/10.1146/annurev.cellbio.24.110707.175347.
3. **Fruh K, Gruhler A, Krishna RM, Schoenhals GJ.** 1999. A comparison of viral immune escape strategies targeting the MHC class I assembly pathway. Immunol. Rev. **168:**157–166. http://dx.doi.org/10.1111/j.1600-065X.1999.tb01290.x.
4. **Lilley BN, Ploegh HL.** 2005. Viral modulation of antigen presentation: manipulation of cellular targets in the ER and beyond. Immunol. Rev. **207:**126–144. http://dx.doi.org/10.1111/j.0105-2896.2005.00318.x.
5. **Burgert HG, Kvist S.** 1985. An adenovirus type 2 glycoprotein blocks cell surface expression of human histocompatibility class I antigens. Cell **41:**987–997. http://dx.doi.org/10.1016/S0092-8674(85)80079-9.
6. **Fruh K, Ahn K, Djaballah H, Sempe P, van Endert PM, Tampe R, Peterson PA, Yang Y.** 1995. A viral inhibitor of peptide transporters for antigen presentation. Nature **375:**415–418. http://dx.doi.org/10.1038/375415a0.
7. **Hill A, Jugovic P, York I, Russ G, Bennink J, Yewdell J, Ploegh H, Johnson D.** 1995. Herpes simplex virus turns off the TAP to evade host immunity. Nature **375:**411–415. http://dx.doi.org/10.1038/375411a0.
8. **Koppers-Lalic D, Reits EA, Ressing ME, Lipinska AD, Abele R, Koch J, Marcondes Rezende M, Admiraal P, van Leeuwen D, Bienkowska-Szewczyk K, Mettenleiter TC, Rijsewijk FA, Tampe R, Neefjes J, Wiertz EJ.** 2005. Varicelloviruses avoid T cell recognition by UL49.5-mediated inactivation of the transporter associated with antigen processing. Proc. Natl. Acad. Sci. U. S. A. **102:**5144–5149. http://dx.doi.org/10.1073/pnas.0501463102.
9. **Koppers-Lalic D, Verweij MC, Lipinska AD, Wang Y, Quinten E, Reits EA, Koch J, Loch S, Marcondes Rezende M, Daus F, Bienkowska-Szewczyk K, Osterrieder N, Mettenleiter TC, Heemskerk MH, Tampe R, Neefjes JJ, Chowdhury SI, Ressing ME, Rijsewijk FA, Wiertz EJ.** 2008. Varicellovirus UL 49.5 proteins differentially affect the function of the transporter associated with antigen processing, TAP. PLoS Pathog. **4:**e1000080. http://dx.doi.org/10.1371/journal.ppat.1000080.
10. **Ma G, Azab W, Osterrieder N.** 2013. Equine herpesviruses type 1 (EHV-1) and 4 (EHV-4)–masters of co-evolution and a constant threat to equids and beyond. Vet. Microbiol. **167:**123–134. http://dx.doi.org/10.1016/j.vetmic.2013.06.018.
11. **Kydd JH, Wattrang E, Hannant D.** 2003. Pre-infection frequencies of equine herpesvirus-1 specific, cytotoxic T lymphocytes correlate with protection against abortion following experimental infection of pregnant mares. Vet. Immunol. Immunopathol. **96:**207–217. http://dx.doi.org/10.1016/j.vetimm.2003.08.004.
12. **Rappocciolo G, Birch J, Ellis SA.** 2003. Down-regulation of MHC class I expression by equine herpesvirus-1. J. Gen. Virol. **84:**293–300. http://dx.doi.org/10.1099/vir.0.18612-0.
13. **Ma G, Feineis S, Osterrieder N, Van de Walle GR.** 2012. Identification and characterization of equine herpesvirus type 1 pUL56 and its role in virus-induced downregulation of major histocompatibility complex class I. J. Virol. **86:**3554–3563. http://dx.doi.org/10.1128/JVI.06994-11.
14. **Said A, Azab W, Damiani A, Osterrieder N.** 2012. Equine herpesvirus type 4 UL56 and UL49.5 proteins downregulate cell surface major histocompatibility complex class I expression independently of each other. J. Virol. **86:**8059–8071. http://dx.doi.org/10.1128/JVI.00891-12.
15. **Goodman LB, Loregian A, Perkins GA, Nugent J, Buckles EL, Mercorelli B, Kydd JH, Palu G, Smith KC, Osterrieder N, Davis-Poynter N.** 2007. A point mutation in a herpesvirus polymerase determines neuropathogenicity. PLoS Pathog. **3:** e160. http://dx.doi.org/10.1371/journal.ppat.0030160.
16. **Tischer BK, von Einem J, Kaufer B, Osterrieder N.** 2006. Two-step red-mediated recombination for versatile high-efficiency markerless DNA manipulation in Escherichia coli. Biotechniques **40:**191–197. http://dx.doi.org/10.2144/000112096.
17. **O'Callaghan DJ, Colle CF, III, Flowers CC, Smith RH, Benoit JN, Bigger CA.** 1994. Identification and initial characterization of the IR6 protein of equine herpesvirus 1. J. Virol. **68:**5351–5364.
18. **von Kleist L, Stahlschmidt W, Bulut H, Gromova K, Puchkov D, Robertson MJ, MacGregor KA, Tomilin N, Pechstein A, Chau N,**

Chircop M, Sakoff J, von Kries JP, Saenger W, Krausslich HG, Shupliakov O, Robinson PJ, McCluskey A, Haucke V. 2011. Role of the clathrin terminal domain in regulating coated pit dynamics revealed by small molecule inhibition. Cell **146:**471–484. http://dx.doi.org/10.1016/j.cell.2011.06.025.

19. **Coscoy L, Ganem D.** 2000. Kaposi's sarcoma-associated herpesvirus encodes two proteins that block cell surface display of MHC class I chains by enhancing their endocytosis. Proc. Natl. Acad. Sci. U. S. A. **97:**8051–8056. http://dx.doi.org/10.1073/pnas.140129797.
20. **Cao H, Thompson HM, Krueger EW, McNiven MA.** 2000. Disruption of Golgi structure and function in mammalian cells expressing a mutant dynamin. J. Cell Sci. **113:**1993–2002.
21. **Benmerah A, Lamaze C, Begue B, Schmid SL, Dautry-Varsat A, Cerf-Bensussan N.** 1998. AP-2/Eps15 interaction is required for receptor-mediated endocytosis. J. Cell Biol. **140:**1055–1062. http://dx.doi.org/10.1083/jcb.140.5.1055.
22. **Stroh T, Erben U, Kuhl AA, Zeitz M, Siegmund B.** 2010. Combined pulse electroporation—a novel strategy for highly efficient transfection of human and mouse cells. PLoS One **5:** e9488. http://dx.doi.org/10.1371/journal.pone.0009488.
23. **Luzio JP, Pryor PR, Bright NA.** 2007. Lysosomes: fusion and function. Nat. Rev. Mol. Cell Biol. **8:**622–632. http://dx.doi.org/10.1038/nrm2217.
24. **Fredericksen BL, Wei BL, Yao J, Luo T, Garcia JV.** 2002. Inhibition of endosomal/lysosomal degradation increases the infectivity of human immunodeficiency virus. J. Virol. **76:**11440–11446. http://dx.doi.org/10.1128/JVI.76.22.11440-11446.2002.
25. **Dutta D, Donaldson JG.** 2012. Search for inhibitors of endocytosis: intended specificity and unintended consequences. Cell Logist. **2:**203–208. http://dx.doi.org/10.4161/cl.23967.
26. **Drose S, Altendorf K.** 1997. Bafilomycins and concanamycins as inhibitors of V-ATPases and P-ATPases. J. Exp. Biol. **200:**1–8.
27. **Doherty GJ, McMahon HT.** 2009. Mechanisms of endocytosis. Annu. Rev. Biochem. **78:**857–902. http://dx.doi.org/10.1146/annurev.biochem.78.081307.110540.
28. **Macia E, Ehrlich M, Massol R, Boucrot E, Brunner C, Kirchhausen T.** 2006. Dynasore, a cell-permeable inhibitor of dynamin. Dev. Cell **10:**839–850. http://dx.doi.org/10.1016/j.devcel.2006.04.002.
29. **Wang LH, Rothberg KG, Anderson RG.** 1993. Mis-assembly of clathrin lattices on endosomes reveals a regulatory switch for coated pit formation. J. Cell Biol. **123:**1107–1117. http://dx.doi.org/10.1083/jcb.123.5.1107.
30. **Benmerah A, Bayrou M, Cerf-Bensussan N, Dautry-Varsat A.** 1999. Inhibition of clathrin-coated pit assembly by an Eps15 mutant. J. Cell Sci. **112:**1303–1311.
31. **Nabi IR, Le PU.** 2003. Caveolae/raft-dependent endocytosis. J. Cell Biol. **161:**673–677. http://dx.doi.org/10.1083/jcb.200302028.
32. **Schnitzer JE, Oh P, Pinney E, Allard J.** 1994. Filipin-sensitive caveolae-mediated transport in endothelium: reduced transcytosis, scavenger endocytosis, and capillary permeability of select macromolecules. J. Cell Biol. **127:**1217–1232. http://dx.doi.org/10.1083/jcb.127.5.1217.
33. **Chen Y, Wang S, Lu X, Zhang H, Fu Y, Luo Y.** 2011. Cholesterol sequestration by nystatin enhances the uptake and activity of endostatin in endothelium via regulating distinct endocytic pathways. Blood **117:**6392–6403. http://dx.doi.org/10.1182/blood-2010-12-322867.
34. **Mundy DI, Li WP, Luby-Phelps K, Anderson RG.** 2012. Caveolin targeting to late endosome/lysosomal membranes is induced by perturbations of lysosomal pH and cholesterol content. Mol. Biol. Cell **23:**864–880. http://dx.doi.org/10.1091/mbc.E11-07-0598.
35. **Vercauteren D, Vandenbroucke RE, Jones AT, Rejman J, Demeester J, De Smedt SC, Sanders NN, Braeckmans K.** 2010. The use of inhibitors to study endocytic pathways of gene carriers: optimization and pitfalls. Mol. Ther. **18:**561–569. http://dx.doi.org/10.1038/mt.2009.281.
36. **Orlichenko L, Huang B, Krueger E, McNiven MA.** 2006. Epithelial growth factor-induced phosphorylation of caveolin 1 at tyrosine 14 stimulates caveolae formation in epithelial cells. J. Biol. Chem. **281:**4570–4579. http://dx.doi.org/10.1074/jbc.M512088200.
37. **Shatz M, Lustig G, Reich R, Liscovitch M.** 2010. Caveolin-1 mutants P132L and Y14F are dominant negative regulators of invasion, migration and aggregation in H1299 lung cancer cells. Exp. Cell Res. **316:**1748–1762. http://dx.doi.org/10.1016/j.yexcr.2010.02.006.
38. **Pelkmans L, Kartenbeck J, Helenius A.** 2001. Caveolar endocytosis of simian virus 40 reveals a new two-step vesicular-transport pathway to the ER. Nat. Cell Biol. **3:**473–483. http://dx.doi.org/10.1038/35074539.
39. **Duncan LM, Piper S, Dodd RB, Saville MK, Sanderson CM, Luzio JP, Lehner PJ.** 2006. Lysine-63-linked ubiquitination is required for endolysosomal degradation of class I molecules. EMBO J. **25:**1635–1645. http://dx.doi.org/10.1038/sj.emboj.7601056.
40. **Ushijima Y, Luo C, Kamakura M, Goshima F, Kimura H, Nishiyama Y.** 2010. Herpes simplex virus UL56 interacts with and regulates the Nedd4-family ubiquitin ligase Itch. Virol. J. **7:**179. http://dx.doi.org/10.1186/1743-422X-7-179.
41. **Yang Y, Kitagaki J, Dai RM, Tsai YC, Lorick KL, Ludwig RL, Pierre SA, Jensen JP, Davydov IV, Oberoi P, Li CC, Kenten JH, Beutler JA, Vousden KH, Weissman AM.** 2007. Inhibitors of ubiquitin-activating enzyme (E1), a new class of potential cancer therapeutics. Cancer Res. **67:**9472–9481. http://dx.doi.org/10.1158/0008-5472.CAN-07-0568.
42. **Liszewski MK, Post TW, Atkinson JP.** 1991. Membrane cofactor protein (MCP or CD46): newest member of the regulators of complement activation gene cluster. Annu. Rev. Immunol. **9:**431–455. http://dx.doi.org/10.1146/annurev.iy.09.040191.002243.
43. **Deckert M, Kubar J, Bernard A.** 1992. CD58 and CD59 molecules exhibit potentializing effects in T cell adhesion and activation. J. Immunol. **148:**672–677.
44. **Pfistershammer K, Majdic O, Stockl J, Zlabinger G, Kirchberger S, Steinberger P, Knapp W.** 2004. CD63 as an activation-linked T cell costimulatory element. J. Immunol. **173:**6000–6008. http://dx.doi.org/10.4049/jimmunol.173.10.6000.
45. **Krammer PH.** 2000. CD95's deadly mission in the immune system. Nature **407:**789–795. http://dx.doi.org/10.1038/35037728.
46. **Hansen TH, Bouvier M.** 2009. MHC class I antigen presentation: learning from viral evasion strategies. Nat. Rev. Immunol. **9:**503–513. http://dx.doi.org/10.1038/nri2575.
47. **Mercer J, Schelhaas M, Helenius A.** 2010. Virus entry by endocytosis. Annu. Rev. Biochem. **79:**803–833. http://dx.doi.org/10.1146/annurev-biochem-060208-104626.
48. **Blagoveshchenskaya AD, Thomas L, Feliciangeli SF, Hung CH, Thomas G.** 2002. HIV-1 Nef downregulates MHC-I by a PACS-1- and PI3K-regulated ARF6 endocytic pathway. Cell **111:**853–866. http://dx.doi.org/10.1016/S0092-8674(02)01162-5.
49. **Ahn K, Meyer TH, Uebel S, Sempe P, Djaballah H, Yang Y, Peterson PA, Fruh K, Tampe R.** 1996. Molecular mechanism and species specificity of TAP inhibition by herpes simplex virus ICP47. EMBO J. **15:**3247–3255.
50. **Tomazin R, Hill AB, Jugovic P, York I, van Endert P, Ploegh HL, Andrews DW, Johnson DC.** 1996. Stable binding of the herpes simplex virus ICP47 protein to the peptide binding site of TAP. EMBO J. **15:**3256–3266.
51. **Mayor S, Pagano RE.** 2007. Pathways of clathrin-independent endocytosis. Nat. Rev. Mol. Cell Biol. **8:**603–612. http://dx.doi.org/10.1038/nrm2216.
52. **Le Roy C, Wrana JL.** 2005. Clathrin- and non-clathrin-mediated endocytic regulation of cell signalling. Nat. Rev. Mol. Cell Biol. **6:**112–126. http://dx.doi.org/10.1038/nrm1571.
53. **Liu P, Rudick M, Anderson RG.** 2002. Multiple functions of caveolin-1. J. Biol. Chem. **277:**41295–41298. http://dx.doi.org/10.1074/jbc.R200020200.
54. **Nomura R, Fujimoto T.** 1999. Tyrosine-phosphorylated caveolin-1: immunolocalization and molecular characterization. Mol. Biol. Cell **10:**975–986. http://dx.doi.org/10.1091/mbc.10.4.975.
55. **Qie L, Marcellino D, Herold BC.** 1999. Herpes simplex virus entry is associated with tyrosine phosphorylation of cellular proteins. Virology **256:**220–227. http://dx.doi.org/10.1006/viro.1999.9673.
56. **Damm EM, Pelkmans L, Kartenbeck J, Mezzacasa A, Kurzchalia T, Helenius A.** 2005. Clathrin- and caveolin-1-independent endocytosis: entry of simian virus 40 into cells devoid of caveolae. J. Cell Biol. **168:**477–488. http://dx.doi.org/10.1083/jcb.200407113.
57. **Mulherkar N, Raaben M, de la Torre JC, Whelan SP, Chandran K.** 2011. The Ebola virus glycoprotein mediates entry via a non-classical dynamin-dependent macropinocytic pathway. Virology **419:**72–83. http://dx.doi.org/10.1016/j.virol.2011.08.009.
58. **Azab W, Lehmann MJ, Osterrieder N.** 2013. Glycoprotein H and alpha4beta1 integrins determine the entry pathway of alphaherpesviruses. J. Virol. **87:**5937–5948. http://dx.doi.org/10.1128/JVI.03522-12.
59. **Hinshaw JE, Schmid SL.** 1995. Dynamin self-assembles into rings suggesting a mechanism for coated vesicle budding. Nature **374:**190–192. http://dx.doi.org/10.1038/374190a0.
60. **Marks B, Stowell MH, Vallis Y, Mills IG, Gibson A, Hopkins CR, McMahon HT.** 2001. GTPase activity of dynamin and resulting confor-

mation change are essential for endocytosis. Nature **410:**231–235. http://dx.doi.org/10.1038/35065645.
61. **Strous GJ, Govers R.** 1999. The ubiquitin-proteasome system and endocytosis. J. Cell Sci. **112:**1417–1423.
62. **Hicke L.** 2001. A new ticket for entry into budding vesicles-ubiquitin. Cell **106:**527–530. http://dx.doi.org/10.1016/S0092-8674(01)00485-8.
63. **Pickart CM, Fushman D.** 2004. Polyubiquitin chains: polymeric protein signals. Curr. Opin. Chem. Biol. **8:**610–616. http://dx.doi.org/10.1016/j.cbpa.2004.09.009.
64. **Means RE, Lang SM, Jung JU.** 2007. The Kaposi's sarcoma-associated herpesvirus K5 E3 ubiquitin ligase modulates targets by multiple molecular mechanisms. J. Virol. **81:**6573–6583. http://dx.doi.org/10.1128/JVI.02751-06.
65. **Ushijima Y, Koshizuka T, Goshima F, Kimura H, Nishiyama Y.** 2008. Herpes simplex virus type 2 UL56 interacts with the ubiquitin ligase Nedd4 and increases its ubiquitination. J. Virol. **82:**5220–5233. http://dx.doi.org/10.1128/JVI.02515-07.
66. **Riley-Vargas RC, Gill DB, Kemper C, Liszewski MK, Atkinson JP.** 2004. CD46: expanding beyond complement regulation. Trends Immunol. **25:**496–503. http://dx.doi.org/10.1016/j.it.2004.07.004.
67. **Cardoso AI, Gerlier D, Wild TF, Rabourdin-Combe C.** 1996. The ectodomain of measles virus envelope glycoprotein does not gain access to the cytosol and MHC class I presentation pathway following virus-cell fusion. J. Gen. Virol. **77:**2695–2699. http://dx.doi.org/10.1099/0022-1317-77-11-2695.
68. **Levy S, Shoham T.** 2005. The tetraspanin web modulates immune-signalling complexes. Nat. Rev. Immunol. **5:**136–148. http://dx.doi.org/10.1038/nri1548.
69. **Pols MS, Klumperman J.** 2009. Trafficking and function of the tetraspanin CD63. Exp. Cell Res. **315:**1584–1592. http://dx.doi.org/10.1016/j.yexcr.2008.09.020.
70. **Engering A, Pieters J.** 2001. Association of distinct tetraspanins with MHC class II molecules at different subcellular locations in human immature dendritic cells. Int. Immunol. **13:**127–134. http://dx.doi.org/10.1093/intimm/13.2.127.
71. **Soboll Hussey G, Hussey SB, Wagner B, Horohov DW, Van de Walle GR, Osterrieder N, Goehring LS, Rao S, Lunn DP.** 2011. Evaluation of immune responses following infection of ponies with an EHV-1 ORF1/2 deletion mutant. Vet. Res. **42:**23. http://dx.doi.org/10.1186/1297-9716-42-23.
72. **Thomas M, Wills M, Lehner PJ.** 2008. Natural killer cell evasion by an E3 ubiquitin ligase from Kaposi's sarcoma-associated herpesvirus. Biochem. Soc. Trans. **36:**459–463. http://dx.doi.org/10.1042/BST0360459.
73. **Nathan JA, Lehner PJ.** 2009. The trafficking and regulation of membrane receptors by the RING-CH ubiquitin E3 ligases. Exp. Cell Res. **315:**1593–1600. http://dx.doi.org/10.1016/j.yexcr.2008.10.026.